FEATURE ARTICLE

Nanosecond and Femtosecond Laser Photochemistry and Ablation Dynamics of Neat Liquid Benzenes

Koji Hatanaka,*,† Yasuyuki Tsuboi,‡ Hiroshi Fukumura,† and Hiroshi Masuhara*,§

Department of Chemistry, Graduate School of Science, Tohoku University, Sendai, Miyagi 980-8578, Japan, Department of Chemistry, Graduate School of Science, Hokkaido University, Sapporo, Hokkaido 060-0812, Japan, and Department of Applied Physics and Frontier Research Center, Osaka University, Suita, Osaka 565-0871, Japan

Received: November 27, 2001

Molecular mechanisms of nanosecond and femtosecond laser ablation and morphology-changing dynamics of neat liquid benzene derivatives, such as benzyl chloride and toluene, were investigated by photoacoustic measurement, nanosecond shadowgraphy, femtosecond surface light scattering imaging, and time-resolved ultraviolet−visible absorption spectroscopy. Ablation thresholds of the liquids were determined by photoacoustic measurement and shadowgraphy, whereas primary processes in ablation were elucidated by time-resolved absorption spectroscopy. Femtosecond surface light scattering imaging revealed how electronic excited/radical states evolved to nanometer morphological changes. In nanosecond laser ablation, ablation threshold value was related to photochemical reactivity producing benzyl radical; however, no correlation between the threshold and boiling point was confirmed. Indeed, a benzyl radical absorption band was clearly observed. Moreover, benzyl radical concentration at the threshold was estimated quantitatively as approximately 0.05 M in accordance with all sample liquids. Consequently, we concluded that nanosecond laser ablation of the liquids is induced photochemically by benzyl radical formation, and not by photothermal temperature elevation. In the case of femtosecond laser ablation, the relation between ablation threshold value and photochemical reactivity did not hold. Time-resolved absorption spectroscopy of liquid benzyl chloride clearly afforded benzyl radical absorption; in contrast, no radical absorption band was observed for toluene. The molecular ablation mechanism of toluene was thought to change into a photothermal mechanism upon application of femtosecond excitation. A double-pulse excitation experiment employing toluene demonstrated how the photothermal mechanism in femtosecond laser ablation was changed to the photochemical mechanism in nanosecond ablation.

I. Introduction

Since the introduction of the laser in 1960, specific properties of laser beams, including monochromaticity, high intensity, short pulse, etc., have been recognized as possessing extremely useful characteristics by chemists and have been introduced to various fields of chemistry. In particular, in physical chemistry, the superior performance of monochromaticity and time resolution has received much attention. State-to-state chemistry, ultrafast chemistry, etc., constitute the mainstream in laser chemistry.[1] It is possible to excite molecules into selected rotational, vibrational and electronic states in order to probe the following relaxation and decomposition dynamics, and to identify the final states of resultant products. All such studies are based on developments in high-resolution laser spectroscopy. Primary chemical events occurring in nanosecond, picosecond and femtosecond time domains are also clarified by time-resolved absorption spectroscopy as well as fluorescence spectroscopy. In some instances, transient grating spectroscopy is utilized.[2]

It is worth noting that spectroscopic measurements in a wide range of wavelengths, which make possible the identification of unrelaxed and relaxed excited states, ionic and neutral radicals, metastable species, and final products, have played the most important roles in ultrafast chemistry. A dynamic analysis at one wavelength is effective only when the species or states probed can be assumed. Processes such as electron transfer, proton transfer, energy transfer, isomerization, and decomposition have been elucidated in detail by time-resolved absorption spectroscopy. Of course, targets have expanded from solution and gas phases to colloid and biological systems. Furthermore, functional materials, such as films, crystalline powders, and microparticles, have recently been studied by ultrafast reflection spectroscopy.[3]

The important feature of laser light, which is emphasized here, is its high intensity. Laser pulses are readily focused into small areas where numbers of photons and molecules are in the same order. Studies regarding interactions between such intense laser pulses and molecules have recently entered the mainstream in laser chemistry beyond conventional photophysics and photochemistry. Various nonlinear processes have been clarified for isolated molecules and clusters in the gas phase.[4] On the other

* Authors to whom all correspondence should be addressed. E-mails: hatanaka@orgphys.chem.tohoku.ac.jp; masuhara@ap.eng.osaka-u.ac.jp.
† Tohoku University.
‡ Hokkaido University.
§ Osaka University.

10.1021/jp014332h CCC: $22.00
Published on Web 02/26/2002

hand, in condensed matter, intense laser pulse excitation induces not only multiphoton excitation phenomena but also heating, vaporization and expansion. Laser ablation is a phenomenon commonly induced in solids and liquids as a result of such interactions. Thus, elucidation of the mechanism by which intense laser excitation evolves to morphological change is believed to be indispensable and of great import.

From this perspective, we have investigated laser ablation as a representative of unconventional phenomena and clarified its molecular mechanisms and macroscopic morphology-changing dynamics over the past decade.[9−19] Initially, we summarize relevant results pertaining to laser ablation of polymer solids and aromatic molecule-doped polymer films. Several representative studies were first reported by Srinivasan et al.[5] and Namba et al.[6] in 1982. These mechanisms have been widely investigated over the past fifteen years. From the perspective of photochemistry and photophysics, two possible models have been proposed to date mainly for interpretation of aromatic molecule-doped polymer ablation by ultraviolet (UV) laser pulses: photochemical and photothermal mechanisms. The former represents a model in which ablation is induced by instantaneous volume explosion triggered by photochemically produced radicals,[7] while the latter is based on a model where ablation is induced by explosive boiling induced by instantaneous temperature elevation.[8]

To understand laser ablation in terms of photophysics and photochemistry, we have started our study by choosing polymer films doped with aromatic molecules, such as pyrene,[9−12] biphenyl,[11] porphyrins,[12,13] and so on, as their photophysics and photochemistry have been already clarified well. It was considered to be indispensable to monitor the dynamics of electronic excited states and reaction intermediates with time-resolved spectroscopy and to bridge the gap between molecular-scaled phenomena and macroscopic morphological changes. Morphology-changing dynamics has been studied by using time-resolved shadowgraphy[14] and interferometry[15] and combined with dynamic spectroscopic data to clarify laser ablation mechanisms from the molecular viewpoints. Examining of the experimental conditions of most ablation studies, we consider that the past studies have revealed that laser ablation of most polymers is initiated by photothermal temperature elevation. For polymer films doped with laser-absorbing aromatic molecules, we have demonstrated the mechanism by which absorbed energy is converted into the thermal mechanism: cyclic multiphotonic absorption[16] of laser light by excited states and transient species such as ions and radicals. The photothermal effect was confirmed even in cases involving polymer films doped with photochemically active molecules, such as 5-diazo-2,2-dimethyl-1,3-dioxane-4,6-diodine (5-diazo Meldrum's acid)[17] and *N*,*N*,*N*′,*N*′-tetramethyl-*p*-phenylenediamine.[18] On the other hand, distinct photochemical ablation is limited to triazene polymers where a photoreactive triazeno group is bonded in primary chains.[19] In the case of polymers, however, the structures are microscopically inhomogeneous due to conformation, tacticity, cross-linking, molecular weight distribution, etc. In particular, under laser ablation conditions, bond breaking, intra- and intermolecular thermal energy dissipation, and ejection of fragments with different masses can be coupled with one another. These possibilities lend complexity to the laser ablation mechanism. As a result, direct correlation between photochemical processes and laser ablation remains ambiguous to some extent.

Separately from practical applications, molecular organic liquids such as benzene derivatives serve as one of the best systems in terms of elucidation of ablation mechanisms as these molecules possess a comparatively simple structure, in addition to displaying microscopic homogeneity and isotropic nature; moreover, chemical bonds are not formed between molecules. These characteristics are favorable with respect to elucidation of ablation mechanisms and bridging of the gap between molecular mechanisms and morphological changes. Indeed, photochemistry of benzene derivatives has been widely investigated as the standard large molecules in the past several decades. Thus, liquid benzene derivatives, including benzyl chloride and toluene, have been adopted in the present study as sample liquids. Moreover, various nanosecond and femtosecond pump−probe methods have been developed and utilized under laser ablation conditions in this investigation.

Photochemistry and photophysics of benzene derivatives have been extensively studied; additionally, innumerable reports appear in the literature and are summarized briefly as follows. In the gas phase, higher excited states generated by laser excitation are converted into highly vibrationally excited and electronic ground states. Subsequently, hot molecules are produced. For instance, Nakashima et al.[20] reported the process under nanosecond 193 nm laser pulse excitation conditions. Troe et al. also documented the process under shock wave pulse excitation conditions[21] and nanosecond laser excitation conditions.[22] Those reports suggested a "hot molecule mechanism"[23] as a benzyl radical formation process. The hot molecules appear to be related to laser ablation of neat liquids induced by high density photons; however, intermolecular interactions in neat liquids accelerate energy dissipation, such that temperature elevation should occur instead of hot molecules formation. Even in a condensed phase similar to the present study, it is generally accepted that benzene derivatives are reactive to UV light excitation and produce benzyl radical as follows:

$$\phi\text{-}CH_2X + h\nu\ (UV) \rightarrow \phi\text{-}CH_2\bullet + X\bullet \qquad (1)$$

Relative reactivity among these liquids has been documented by Porter et al.[24] as follows:

$$\phi\text{-}CH_2Cl,\ \phi\text{-}CH_2OH > \phi\text{-}CH_3 > \phi\text{-}C_2H_5,\ \phi\text{-}C_3H_7 \qquad (2)$$

Furthermore, excited states of generated benzyl radicals have been investigated in detail as its doublet−doublet transition has received much attention.[25] It is noteworthy that physical parameters of the liquids (molar absorption coefficient, ionization potential, energy level of excited state, heat capacity, etc.) are nearly identical due to their analogous molecular and electronic structures. Thus, these liquids appear indeed suitable for the study of laser ablation molecular mechanisms from a photochemical perspective.

This paper describes laser photochemistry and ablation dynamics of neat liquid benzenes. Organization is as follows. In section II, sample liquids and experimental techniques for laser ablation studies are summarized briefly. In section III, the study of nanosecond laser ablation is presented. Ablation threshold values are estimated in section IIIa by photoacoustic measurement. In addition, the relation of threshold values is investigated primarily from the perspectives of reactivity and temperature elevation. Following in section IIIb, results obtained employing time-resolved spectroscopy are displayed and the formation of transient species, i.e., benzyl radical, is confirmed. Further, benzyl radical concentration is quantitatively estimated at ablation thresholds and verification of the photochemical laser ablation mechanism is attained. The study regarding femtosecond laser ablation and examination of its molecular mechanism are described in section IV. In section IVa, we introduce a novel

imaging method and apply it to femtosecond laser ablation for the investigation of initial morphological changes with picosecond time resolution. In terms of roughness analysis, we attempt to quantify the initial stage of morphological changes in nanometer spatial resolution. Subsequently, in section IVb, results obtained by time-resolved absorption spectroscopy are presented and discussed in terms of the benzyl radical formation process, which is the key factor with respect to analysis of laser ablation molecular mechanisms of the sample liquids. Finally, in section V, molecular mechanisms of nanosecond and femtosecond laser ablation and morphological-changing dynamics are summarized.

II. Experimental Section

Benzene derivatives employed in the investigation of nanosecond laser ablation consisted of benzyl compounds, including benzyl chloride (ϕ-CH_2Cl, ϕ represents a phenyl group) and benzyl alcohol (ϕ-CH_2OH), and alkylbenzenes, including toluene (ϕ-CH_3), ethylbenzene (ϕ-C_2H_5), and *n*-propylbenzene (ϕ-C_3H_7). In femtosecond laser ablation experiments, benzyl chloride and toluene were adopted as representative liquid samples of the benzyl compounds and the alkylbenzene derivatives, respectively. All samples were utilized following N_2 bubbling for several minutes; moreover, all liquids were stirred continuously during the experiments in order to avoid exciting photoproducts. Experiments were conducted at ~294 K under an N_2 atmosphere at atmospheric pressure.

A conventional KrF excimer laser (248 nm, 30 ns) was employed as the excitation light source in the study of nanosecond laser ablation. An excitation laser pulse, focused by means of a lens through a square aperture, irradiated the sample surface in order to induce laser ablation where the spot size was 1×1 mm^2. Laser intensity was varied using various transmittance attenuators and measurements were performed with a joule meter. Laser fluence, F, was calculated by the equation $F =$ laser intensity/spot size. Sound waves induced by laser pulse irradiation were detected by a piezoelectric transducer (PZT) attached to the bottom of a sample glass container with silicone grease.[26] Sound intensity was amplified by an electrical circuit and measured by an oscilloscope. Time-resolved UV−visible absorption spectroscopy was conducted with a streak camera system.[26,27]

The excitation light source in the study of femtosecond laser ablation was a Ti^{3+}:Al_2O_3/KrF hybrid laser (248 nm, 300−500 fs). Irradiation conditions were similar to those in the case of nanosecond laser ablation. Additionally, a white light continuum was obtained by focusing the second harmonic (372 nm, 150 fs) into a D_2O cell through a variable optical delay line (19 ns at longest). The continuum was utilized as a strobe light in the scattering imaging and as a probe in pump−probe absorption spectroscopy. In scattering imaging,[28] a white light continuum, functioning as a strobe light, irradiated a sample liquid-free surface vertically downward where an excitation laser pulse irradiated. Backscattered light from the spot was imaged by a lens onto a charge-coupled device (CCD). In absorption spectroscopy,[29,30] multichannel photodiode arrays equipped with polychromators were used as detectors.

III. Nanosecond Photochemistry and Laser Ablation

IIIa. Ablation Threshold Values Correlated to Photochemical Reactivity. The most primary, characteristic, and significant parameter in the study of laser ablation is ablation threshold, F_{th}. In the case of solids such as polymers and metals, an etch depth measurement is the most widely employed method for this purpose. In the case of liquids, however, a static contact measurement method of this nature cannot be conducted as morphological changes are essentially transient. Consequently, time-resolved shadowgraphy[26] was adopted as a dynamic noncontact measurement method to estimate F_{th} values. Rough values were obtained through verification of the occurrence of surface expansion; estimated F_{th} values were 25−35 mJ/cm^2 for benzyl chloride, 60−80 mJ/cm^2 for benzyl alcohol, 24−34 mJ/cm^2 for toluene, 45−55 mJ/cm^2 for ethylbenzene, and 55−65 mJ/cm^2 for *n*-propylbenzene, respectively. To determine the F_{th} values precisely, photoacoustic measurements were conducted,[26] which detected the sound wave (photoacoustic signal) and measured its intensity as a function of F.

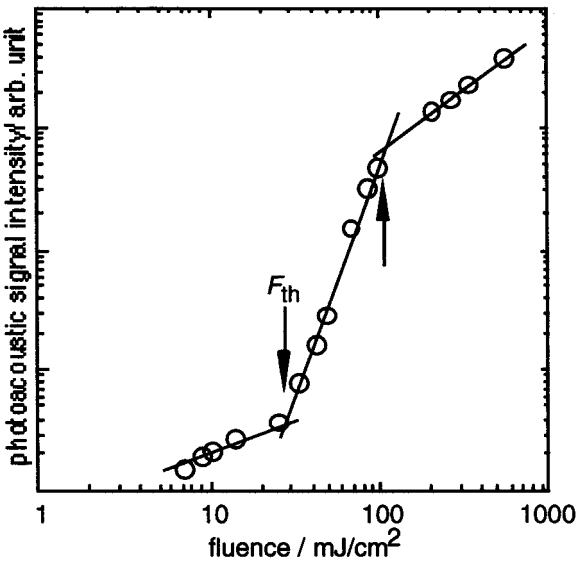

Figure 1. Photoacoustic signal intensity plotted as a function of laser fluence. The sample was liquid benzyl chloride. The arrows represent two break points where the photoacoustic intensity slope changed.

Figure 1 displays results of liquid benzyl chloride as a representative example. All sample liquids demonstrated analogous characteristic behavior; two break points were clearly observed, which are indicated in the figure by arrows. Photoacoustic signal intensity increased gradually in the range of lower F and rose abruptly at the first break point, indicated by a downward arrow. When F continued to increase, the slope of photoacoustic signal intensity again changed gently (break point is indicated by an upward arrow in the figure). The F value at the second break point, which is ~100 mJ/cm^2 in the case of benzyl chloride, was coincident with the F value at which the surface expansion began within the excitation laser pulse width. This observation implies that the slope change at the second break point is due to the shield effect by ejected plume, where the incident excitation laser pulse was absorbed and/or scattered by the plume, and not absorbed by the liquid surface. This phenomenon results in a relative decrease of photoacoustic signal intensity. Zweig et al.,[31] on the other hand, argued in their study of UV laser ablation of polyimide by a fast photoacoustic measurement that the second break point was due to plasma formation. This report offers one explanation for the second break point as a broad luminescence was observed around 400 nm in time-resolved luminescence spectroscopy at $F = 400$ mJ/cm^2 $\gg F_{th}$ described in the next section, which may be related to plasma formation. There are alternative discussions on the second break point; however, a plausible explanation remains unavailable.

The F value at the first break point, 30 mJ/cm^2 in the case of benzyl chloride, was in close agreement with the estimated F_{th}

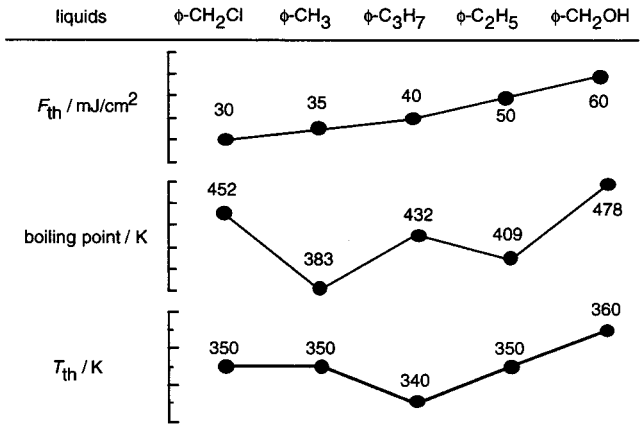

Figure 2. Laser ablation threshold values in nanosecond laser ablation as compared to boiling point and temperature elevation.

value by the shadowgraphy technique described above for each sample liquid; 60 mJ/cm^2 for benzyl alcohol, 35 mJ/cm^2 for toluene, 50 mJ/cm^2 for ethylbenzene, and 40 mJ/cm^2 for *n*-propylbenzene. Therefore, this sudden rise in signal intensity at the first break point was due to the recoil of shock wave generation, plume ejection and surface expansion as related to ablation phenomena; the F value at the first break point was determined as F_{th} for each sample liquid. These F_{th} values are listed in Figure 2 in increasing order from the left side. The order can be examined from various perspectives, including photochemistry, as follows.

First, the relation of F_{th} values from the viewpoint of photochemical reactivity of the sample liquids was examined. As previously described in Introduction, the photochemistry of our sample liquids has been widely studied; moreover, these species are known to produce benzyl radicals under UV light excitation conditions as in (1). The dissociation yield among the liquids is also established as in (2); additionally, the relation of photochemical reactivity is well correlated to the relation of F_{th} values in Figure 2. For instance, the F_{th} value of liquid benzyl chloride is lower than that of liquid toluene as a consequence of the higher reactivity of the former in comparison to that of the latter as in (2). This fact strongly indicates that a photochemical reaction producing benzyl radical should play a key role in nanosecond laser ablation.

Liquid benzyl alcohol is one exception. Its F_{th} value is much higher than that predicted from the relation of photochemical reactivity. In this case, it is probable that intermolecular hydrogen-bonding interactions disturbed the ejection of fragmented products, resulting in the unexpectedly high F_{th} value. Bear in mind that photochemical reactivity cannot be correlated with the bonding energy at the C−X bond in the side chain (β-bond). The bonding energy of ϕCH_2-H (77.5 kcal/mol) is larger than that of ϕCH_2-CH_3 (63 kcal/mol); however, the threshold value of the former is lower than that of the latter. If photothermal dissociation is responsible, the chemical bond possessing lower bond energy should be broken. This finding strongly supports our proposed photochemical mechanism.

Second, a well-known mechanism for laser ablation of liquids and biological tissues involves explosive boiling. This mechanism represents instantaneous temperature elevation; consequently, boiling point serves as the physical parameter with respect to confirmation of ablation induction by this mechanism. A valid mechanism would be characterized by rising F_{th} values correlated with increasing boiling point; however, no such correlation is recognized. For instance, the F_{th} value of liquid benzyl chloride is lower than that of liquid toluene despite the higher boiling point of liquid benzyl chloride (Figure 2). This observation indicates that the explosive boiling mechanism does not apply.

In addition to the qualitative discussion, a quantitative estimation was attempted. The temperature attainable under ablation conditions, T_{th}, can be estimated as follows:

$$T_{th} = 294(\text{room temperature}) + \alpha F_{th}/\rho C \qquad (3)$$

where α is an absorption coefficient, ρ is density and C is the specific heat of the liquid.[13] This determination is valid based on the assumption that the irradiated laser energy is converted entirely into heat, such that the obtained T_{th} is the maximum temperature expected. This value is presented for each sample liquid in Figure 2 with boiling point. Contrary to the case of photochemical reactivity, no correlation exists between T_{th} and F_{th}. Further, T_{th} is much lower than the boiling point for each sample liquid. It is possible for α to change considerably during an excitation laser pulse width under such intense laser pulse irradiation conditions. In time-resolved absorbance measurements (excitation wavelength of 248 nm at $F \sim F_{th}$) conducted separately, however, no significant changes were observed in terms of absorbance at the excitation wavelength for all sample liquids,[27] indicating that α did not change dramatically and that the estimation of T_{th} was valid. This result invalidated the explosive boiling mechanism in the nanosecond laser ablation mechanism of the sample liquids.

Finally, another plausible laser ablation mechanism is the so-called Coulomb explosion.[32,33] Strong repulsive interactions between remaining molecular cations may lead to the explosion. Ejections of electrons from a liquid surface by light irradiation have been frequently reported;[34] however, no correlation exists between ionization potential and F_{th}; the F_{th} value of liquid benzyl chloride is lower than that of liquid toluene despite the higher ionization potential of benzyl chloride (9.2 eV in gas phase[35] versus 8.8 eV in gas phase and 6.9 eV in solution phase,[36] respectively). As a result, the Coulomb explosion mechanism can be discarded as a possible laser ablation mechanism in the present case.

The results and discussion presented above strongly suggest that the nanosecond laser ablation molecular mechanism is photochemical and related to benzyl radical. To inspect the molecular mechanism more precisely, time-resolved luminescence and absorption spectroscopy were conducted. These experiments are described in the next section.

IIIb. Benzyl Radical Formation and Its Concentration under Laser Ablation. To detect transient species such as the benzyl radical under laser ablation conditions, time-resolved luminescence spectroscopy was performed. A representative result, shown in Figure 3, was obtained from liquid benzyl chloride. A band of peak wavelength occurring at ~280 nm was clearly evident in the spectra obtained at $F = F_{th}$ (thin lines) throughout the duration of the observation time range. This band was assigned to the fluorescence of benzyl chloride as it was in close agreement with a reference spectrum.[37] No other significant band was observed at this fluence in the spectra. In the case of higher F, as seen in the spectra of thick lines, on the contrary, the aspects changed dramatically where the F value was 400 mJ/cm^2. At a stage preceding 0 ns, an identical band as described above was observed. With the passage of time, however, several bands which were superimposed on one another were observed: a characteristic sharp band at ~290 nm, a broad band at 250−320 nm, and a second broad band around 400 nm. These bands were observed when F exceeded 200 mJ/cm^2. Benzyl, C_2, CN, and CH radical production was

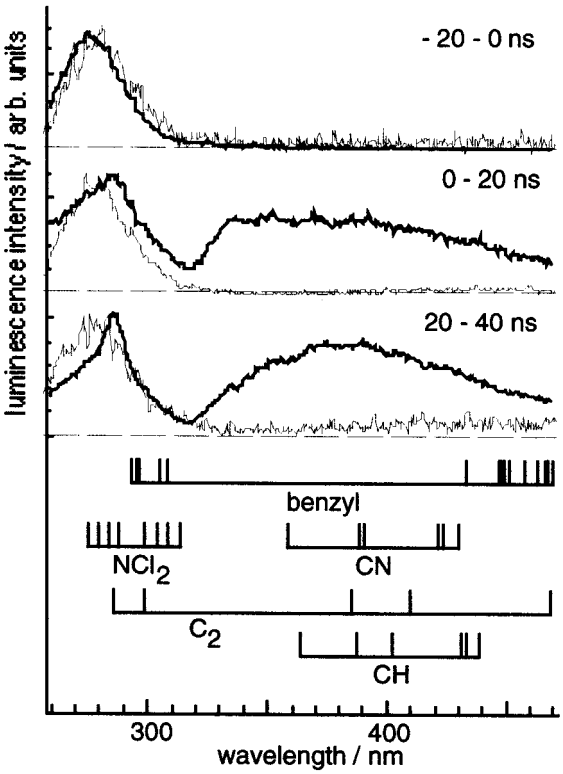

Figure 3. Time-resolved luminescence spectra of liquid benzyl chloride. Spectra in thin lines were obtained when laser fluence was at the threshold (30 mJ/cm^2) and spectra in thick lines were obtained at 400 mJ/cm^2 ($\gg$the threshold). A gate time is noted in each frame. Emission bands of various expected radicals are also shown in the bottom frame.

considered upon comparison of the spectra to references[38] displayed in the bottom of the figure. Presumably, these radicals were efficiently produced due to various chain reactions under a high-intensity irradiation condition. Additionally, a broad band around 400 nm can be attributed to plasma formation as the laser intensity (400 mJ/cm^2) was much higher than the F_{th} value. Interesting information is afforded by luminescence spectroscopy; however, this method does not provide a quantitative basis for analysis of the mechanism.

Rather, time-resolved absorption spectroscopy can identify the main species, which lends itself to greater reliability with respect to elucidation of how these molecular species can initiate ablation. A typical example obtained in this measurement at $F \sim F_{th}$ is shown in Figure 4 (samples were liquid benzyl alcohol in Figure 4a and liquid ethylbenzene in Figure 4b).[30] Although the signal-to-noise ratio is poor as a result of a single-shot measurement of a thin liquid layer under laser ablation conditions, a significant absorption band, peak wavelength at ~320 nm, was commonly observed. This band can be assigned to benzyl radical absorption with absolute certainty due to close agreement with a reference spectrum.[39] The spectroscopic aspects similar to benzyl radical absorption were observed clearly in all sample liquids, which indicates the photochemical mechanism proposed. In addition to the radical absorption band, a broad band over the test wavelength range was also observed. Candidates for the origin of the broad band absorption are the excited singlet and triplet states of the benzene derivatives. Owing to the relatively low extinction coefficient and to spectral broad shape,[40] it is rather difficult to confirm those excited states unless they are produced sufficiently and comparably to the radical. A numerical estimation on the photon numbers absorbed by a molecule at $F = F_{th}$ indicated that only a small percentage of molecules were excited; a bleaching of molecules in the ground state scarcely occurred. Therefore, effects due to absorption by those excited states can be neglected despite their generation. Broad band absorption at late stages can be ascribed to the apparent absorption attributable to scattering of probe light induced by such ablation phenomena. Indeed, the time of surface expansion observed by time-resolved shadowgraphy is consistent with this interpretation.

In addition to the aforementioned qualitative discussions, an evaluation of benzyl radical concentration at $F = F_{th}$ was conducted with the absorbance obtained and Lambert−Beer's law.[27] The concentration of benzyl radical at the irradiated surface, $C_{radical}$, can be derived as follows:

$$C_{radical} = 2.303(\epsilon_{liquid}C_{liquid}/\epsilon_{radical})abs_{radical} \quad (4)$$

where ϵ_{liquid} and C_{liquid} are the molar absorption coefficients in M^{-1} cm^{-1} at the excitation wavelength of 248 nm and the concentration of a liquid (~ 10 M), respectively. $\epsilon_{radical}$ is the molar absorption coefficient of benzyl radical at 318 nm (5500 $M^{-1}cm^{-1}$).[41] $abs_{radical}$ is the maximum transient absorbance at 318 nm obtained in the spectroscopy. $abs_{radical}$ and the estimated $C_{radical}$ values at $F = F_{th}$ are listed in Table 1 together with surface tension of the liquids. Surprisingly, $C_{radical}$ values are similar to one another, ~0.05 M on average; however, F_{th} values and photochemical reactivity change depending on liquids. These findings indicate that the macroscopic morphological changes occurring in time-resolved shadowgraphy are induced when the concentration of the radical reaches a common critical value. Detailed inspection of $C_{radical}$ values permits classification into two groups: one is 0. 046 ± 0.002 M for the alkylbenzene derivatives and the second is 0.055−0.068 M for the benzyl compounds. The difference in the radical concentration may be due to macroscopic liquid properties. One potential candidate is surface tension as macroscopic morphological changes initially require a surface expansion. In actuality, as depicted in Table 1, surface tension of the alkylbenzene derivatives (~28.5 dyn/cm) is lower than that of the benzyl compounds (~38 dyn/cm) as the $C_{radical}$ values of the former are relatively lower than those of the latter. Thus, we concluded that photochemical benzyl radical formation triggers nanosecond laser ablation.

IV. Femtosecond Photochemistry and Laser Ablation

The ablation threshold values of femtosecond laser ablation, determined in a manner similar to nanosecond laser ablation, were 30 mJ/cm^2 for liquid benzyl chloride and 25 mJ/cm^2 for liquid toluene,[42] respectively. It is surprising that the relation between the threshold values (benzyl chloride > toluene) is opposite to that of nanosecond laser ablation (benzyl chloride < toluene). Moreover, this phenomenon cannot be explained in terms of the relation of photochemical reactivity described in (2). This finding suggests that the molecular mechanism of femtosecond laser ablation is distinct from that of nanosecond laser ablation. The nanosecond study has clarified the importance of the role of benzyl radical in laser ablation of liquids, whereas benzyl radical formation and its decay processes remain unknown. Femtosecond photochemistry and laser ablation were investigated employing an ultrafast laser system, a novel time-resolved imaging method and time-resolved absorption spectroscopy. These techniques clearly demonstrated that the ablation mechanism changes dramatically relative to the nanosecond laser ablation.

IVa. Primary Processes of Laser Ablation. In the case of nanosecond laser ablation studies, shadowgraphy was applied

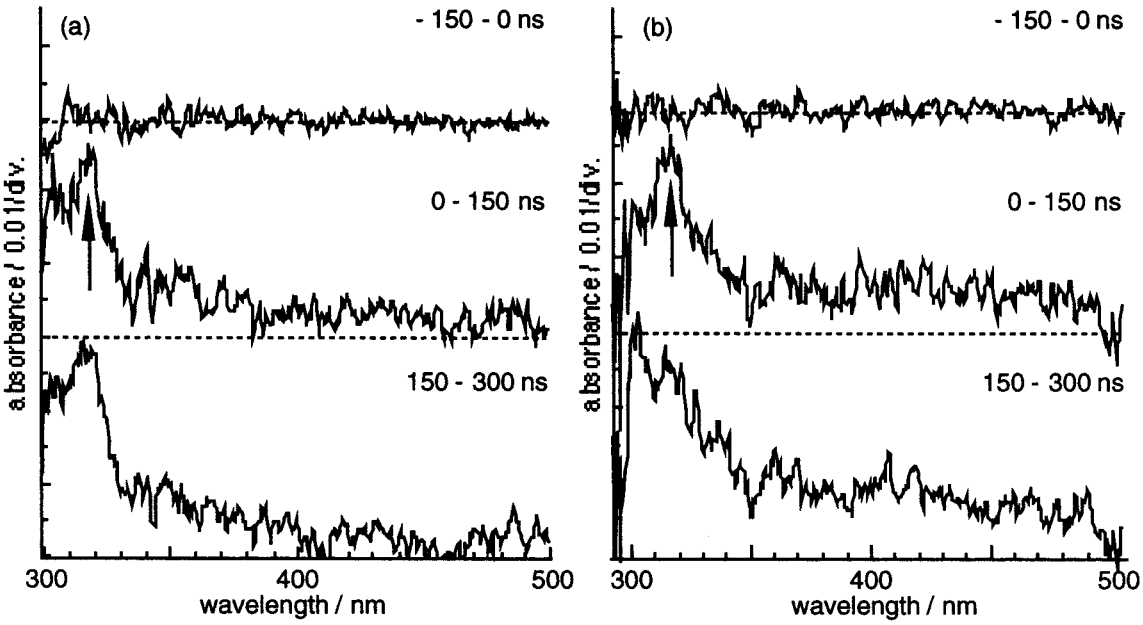

Figure 4. Time-resolved absorption spectra when laser fluence was at the threshold (F_{th}). Sample liquids are (a) benzyl alcohol ($F_{th} = 60$ mJ/cm^2) and (b) ethylbenzene ($F_{th} = 50$ m J/cm^2), respectively. A gate time is noted in each frame. Upward arrows represent a reported absorption band of the benzyl radical.

TABLE 1: Maximum Absorbance of Benzyl Radical at 318 nm and Its Concentration at the Irradiated Liquid Surface near Ablation Threshold Values

liquids	ϕ-CH_2Cl	ϕ-CH_2OH	ϕ-CH_3	ϕ-C_2H_5	ϕ-C_3H_7
$abs_{radical}$	0.17	0.16	0.10	0.14	0.14
$C_{radical}$/M	0.068	0.055	0.044	0.048	0.046
$\gamma/10^{-4}$ N/m	3.7	4.0	2.9	2.9	2.8
$\eta/10^{-4}$ s kg/m	15	78	5.9	6.8	7.9

in order to observe morphological changes. The identical experiment was also performed for femtosecond laser ablation. Results are shown in Figure 5 where the sample liquid was toluene and $F = 90$ mJ/cm^2. As seen in nanosecond laser ablation,[26,27,43] an expanding hemispherical shock wave, gaslike plume and droplets were clearly observed. In addition to these characteristic phenomena, in the femtosecond laser ablation of toluene, a jet expanding vertically upward was observed in the early stages. Its direction was dependent on the incoming direction of laser pulses. A similar jet was not evident in benzyl compounds such as benzyl chloride and benzyl alcohol; however, it was present in alkylbenzenes such as ethylbenzene. One possible interpretation is that the jet arose due to refractive index changes induced by absorption of a laser pulse by ejected vapor. Vapor pressure of the alkylbenzenes (3−22 Torr) is comparatively higher than that of benzyl compounds (0.1−1 Torr). Moreover, the expanding jet was fully disappeared when nitrogen gas flow was applied over the liquid surface, so that we have concluded that the jet was ascribed to refractive index change induced by ionization of vapor.

In addition to shadowgraphy, we have developed a novel time-resolved surface scattering imaging method and observed the initial surface morphological changes with higher temporal resolution using femtosecond pulses as a strobe light.[28] Further, with roughness analysis, higher spatial resolution can be obtained with as little as a few tens of nanometers simultaneously. A typical example of sequential backscattered light images is displayed in Figure 6, where the sample is liquid toluene and $F = 90$ mJ/cm^2. Clear images were not obtained at 0 ps and in the ensuing picosecond time domain. At ~1 ns, a scattered light image from the excitation spot was acquired and its intensity increased with the passage of time. The light and shade in the spots are due to the spatial intensity irregularity of an excitation laser pulse. This transient behavior indicates that the surface scattering is induced by surface morphological changes, not by a transient refractive index change. This premise was confirmed by femtosecond absorption spectroscopy as described in the next section. Briefly, transient absorption of molecular excited states and radicals, which may lead to the refractive index change, was already present at 0 ns. Consequently, the initial stage of surface morphological changes is considered to be the generation of irregular height distribution, i.e., a rugged surface, whereas a flat surface displacement due to expansion/contraction of liquids does not induce such scattering.

At this juncture, backscattered light intensity, I_{scat}, was plotted against the delay time. The results are summarized as a function of F in Figure 7, where the liquids benzyl chloride and toluene are presented Figure 7, parts a and b, respectively. When F was relatively low ($F = 10$ mJ/cm^2), no detectable images were obtained until 19 ns common to both liquids. As F increased above 25 mJ/cm^2, however, backscattered light intensity provided a remarkable count. When initiation of scattering is dependent on the F value, the greater F is, the earlier the starting time. Further, the increasing intensity slope is also dependent on F; the higher the F value, the increasingly steeper the slope. In the case of higher F, saturation and fluctuation of scattered light intensity are observed at the late stage, which may be due to the fact that ejected plumes detaching from a liquid surface shut out the incident probe light pulse and its intensity reaching a liquid surface is decreased as a result. The rise time of backscattered light intensity in benzyl chloride appears to be faster than that of toluene. This occurrence is not due to the macroscopic properties of the liquid, i.e., surface tension and viscosity, since these coefficients for benzyl chloride are larger than those for toluene (Table 1). One interpretation can be based on a difference with respect to benzyl radical production dynamics. That is, a direct bond scission into the benzyl radical may occur in benzyl chloride in the picosecond time range; in

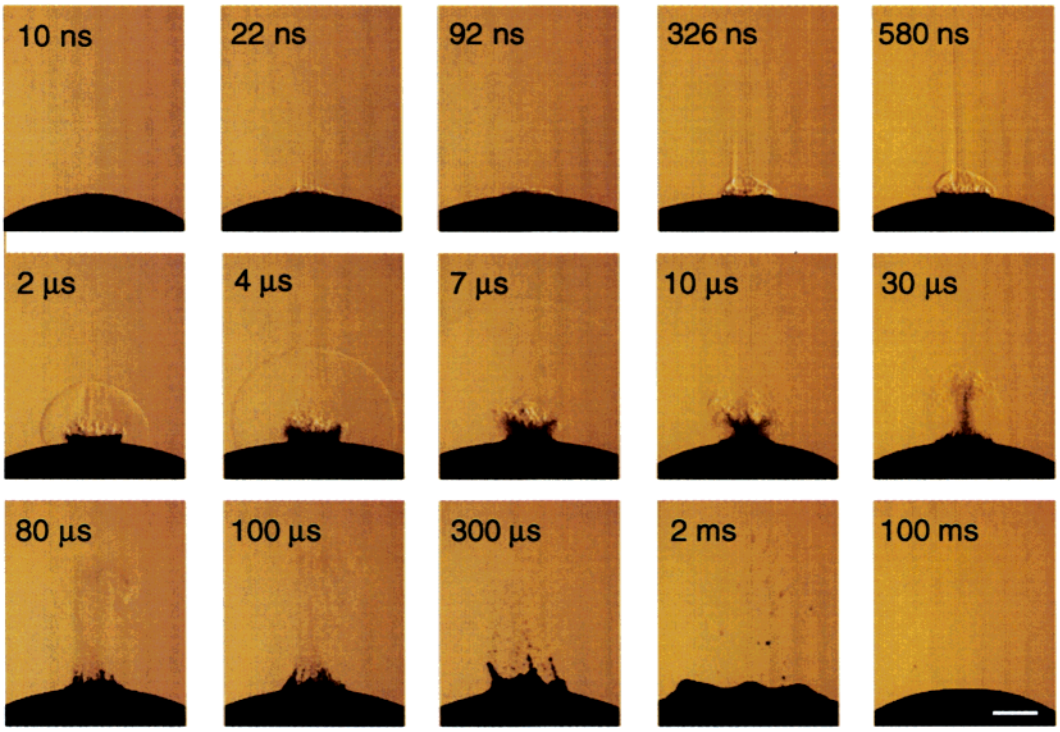

Figure 5. Sequential images under femtosecond laser ablation of liquid toluene at laser fluence of 90 mJ/cm^2. A hemispherical black substance evident in the bottom of each frame represents a swelled liquid-free surface observed from the side. An excitation laser pulse was incident vertically downward to the free surface at 0 ns. A time in each frame represents the observation delay time. A white bar in the last frame represents a scale of 1 mm.

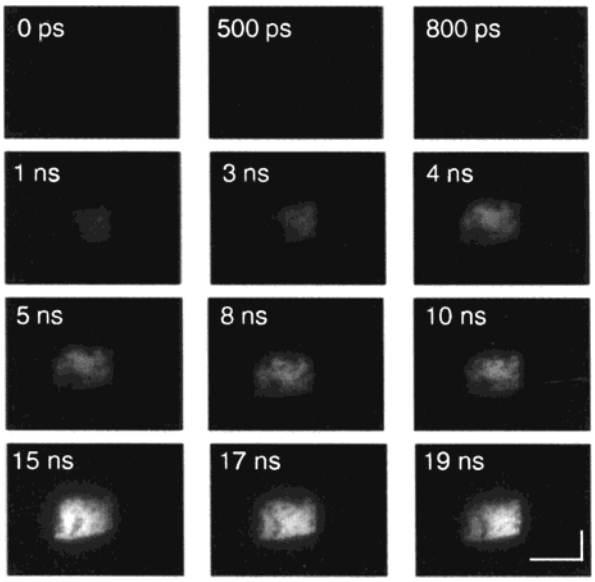

Figure 6. Sequential backscattered light images obtained by CCD when the sample liquid was toluene and laser fluence was 90 mJ/cm^2. A time in each frame represents an observation delay time. The vertical and horizontal white bars in the last frame represent 1 mm. The excitation spot is evident as a parallelogram to some extent as the CCD observed the spot obliquely from above.

contrast, instantaneous bond scission scarcely occurs in toluene (which will be described in the following section).

To extract further quantitative information from the result, the height distribution of a rugged surface as surface roughness was obtained. Additionally, I_{scat} was converted to root-mean-square surface roughness, R_{rms}, under the assumption that the scattering is due exclusively to a rugged surface in this time domain. The relation between backscattered light intensity and surface roughness has been reported as follows under conditions that R_{rms} is small relative to the probe light wavelength, λ, and correlation length in the lateral direction is larger than λ.[44,45]

$$R_{dif} = R_0 (4\pi R_{rms}/\lambda)^2 \quad (5)$$

where R_{dif} is the total diffuse reflectance of a rough surface, and R_0 is the specular reflectance of a perfectly smooth surface of a sample liquid. In cases where backscattering is isotropic to the hemisphere, the equation,

$$I_{scat} = R_{dif}\text{const} \quad (6)$$

is valid. Frosted fused-silica plates are employed as reference samples for the evaluation of surface roughness. R_{rms} values of those plates are measured separately by a stylus profiler characterized by vertical and lateral spatial resolution of 3 and 500 nm, respectively. Subsequently, these results are correlated to I_{scat}. This correlation can be utilized to estimate transient R_{rms} values of the sample liquids. R_{rms} values are shown on the right vertical axes of Figure 6. Estimated R_{rms}, the standard deviation of surface local height, is noticeably on the order of several hundred nanometers.

Based on results obtained by time-resolved imaging methods, morphology-changing dynamics in femtosecond laser ablation can be summarized as follows. Following laser pulse excitation, no morphological changes are induced dramatically until ~1 ns. During this period, specific photochemistry and/or photophysivs occur, which are described in the next section. At approximately 1 ns, a rugged surface characterized by a height of approximately several tens of nanometers is produced. With the passage of time, roughness expands by several hundred nanometers to about 10 ns. Subsequently, surface expansion, shock wave generation and plume and droplet ejection are induced.

IVb. Benzyl Radical Formation Processes and Ablation Molecular Mechanisms. Femtosecond time-resolved absorption

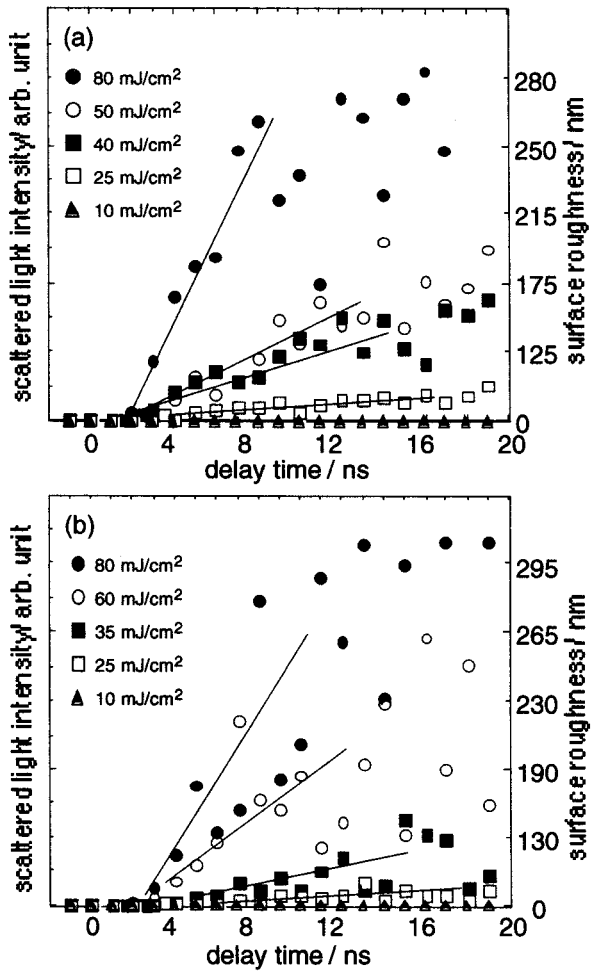

Figure 7. Backscattering light intensity as a function of delay time. Samples were (a) liquid benzyl chloride and (b) liquid toluene. The legends in each figure represent laser fluences. The solid lines serve as a visual aid.

spectra of liquid benzyl chloride are displayed in Figure 8 with different F values and time domains. A rather broad band exhibiting a peak at ~ 320 nm was clearly observed immediately following excitation; moreover, this band was independent of the F values. This band can be assigned to an absorption band of benzyl radical produced as it is in good agreement with a reference spectrum[41] and the nanosecond data presented in Figure 4. When the F value was relatively low at 6 mJ/cm^2, as shown in Figure 8a, a precursor state, i.e., S_1 excited state, was not detected. This observation strongly indicates that benzyl radical is produced via an ultrafast dissociation process, which is consistent with the small fluorescence quantum yield[46] of benzyl chloride even in solid matrix (~0.1). Further, formation of a vibrationally excited state of benzyl radical is not remarkable, as a relaxation process showing vibrational cooling was unclear. This phenomenon is also consistent with a report regarding gas-phase experiments under nanosecond laser pulse excitation conditions where such sharpening was observed by 193 nm pulse irradiation,[47] but not by 266 nm pulse irradiation.[48] The decay dynamics of benzyl radical in the solution phase have been documented solely in the microsecond time range,[39] whereas decay in the picosecond time domain was observed without appreciable spectroscopic change where benzyl radical absorption decreased to 50% of its original level at 0 ns. This decay may be due to geminate and homogeneous recombination processes. Although the latter recombination may produce dibenzyl and chlorine molecules, it is difficult to observe molecular chlorine spectroscopically due to its small extinction coefficient;[49] moreover, distinction of dibenzyl from other species, such as ions and dimers, presents difficulties.

When the F value is sufficiently high, 90 mJ/cm^2 as in Figure 8 (b) and (c), other spectroscopic components were observed. At 0 ns and later, as illustrated in Figure 7(b), a broad band was observed over the observation wavelength range. Its origin can be $S_n \leftarrow S_1$[40] and/or $T_n \leftarrow T_1$ absorption bands. This broad band was observed only when the F value was much higher than F_{th}; consequently, the origin of the broad band may be transient by high-intensity excitation such as benzyl chloride radical cation.[50] In the later stages of the nanosecond time domain as shown in Figure 8c, following complete decay of benzyl radical absorption at 1 ns, a second broad band tailing to the longer wavelength was observed. The absorbance increased with time. This situation was observed exclusively when the F value exceeded F_{th}. Consideration of the induction of surface roughness at ~1 ns (Figure 7a) and correspondence of dynamics to spectral change led to the conclusion that this broad band observed after 1 ns was attributable to probe light scattering as a result of the morphological changes, in addition to surviving residual benzyl radical.

Benzyl radical was produced via an ultrafast pre-dissociation process of benzyl chloride during the time resolution of the measurement system (1.5 ps). Heat generation induced by nonradiative relaxation of benzyl radical excited states is unlikely as the radical cannot absorb an additional photon where dissociation occurred following excitation pulse (300 fs) in 1.5 ps. Even where dissociation occurred during the pulse width (<300 fs), effective heat generation induced by the cyclic multiphoton absorption process[16] by benzyl radical is also unlikely as the lifetime of an excited state of a benzyl radical in solution[39] (~770 ps) is much longer than the excitation pulse width.

The F_{th} value of benzyl chloride was determined as 30 mJ/cm^2 as described. This value is identical to that obtained for nanosecond laser ablation (section III). Benzyl radical absorption in femtosecond and nanosecond laser ablation as a function of F is plotted in Figure 9. At $F = F_{th}$, the absorbance of benzyl radical observed at the delay time of 1 ns is identical to the maximum absorbance observed in nanosecond laser ablation. Further, the slope of absorbance to F is nearly unity in the lower fluence range (<20 mJ/cm^2), which indicates that benzyl radical is produced via a one-photon process even under femtosecond laser excitation conditions. These results indicate that the concentration of benzyl radical produced is dependent only on photon number, and not on laser pulse width; moreover, benzyl radical is produced via an ultrafast dissociation process. Significant temperature elevation was not observed during spectroscopy; therefore, it is believed that the femtosecond laser ablation molecular mechanism of liquid benzyl chloride can be explained with a photochemical process; that is, it is a volume expansion model.

In the case of liquid toluene, the spectroscopic aspects were vastly altered relative to the case of liquid benzyl chloride. Figure 10 displays representative results obtained for liquid toluene and F values of 15 mJ/cm^2 (a) and 60 mJ/cm^2 (b), respectively. A flat absorption covering the observation wavelength range was obtained at the early delay time following laser excitation for F values. This absorption can be S_1, T_1, or the excimer of toluene and/or ions (discussed later). The most outstanding difference between the two series of spectra at different F values is the spectral features of the nanosecond

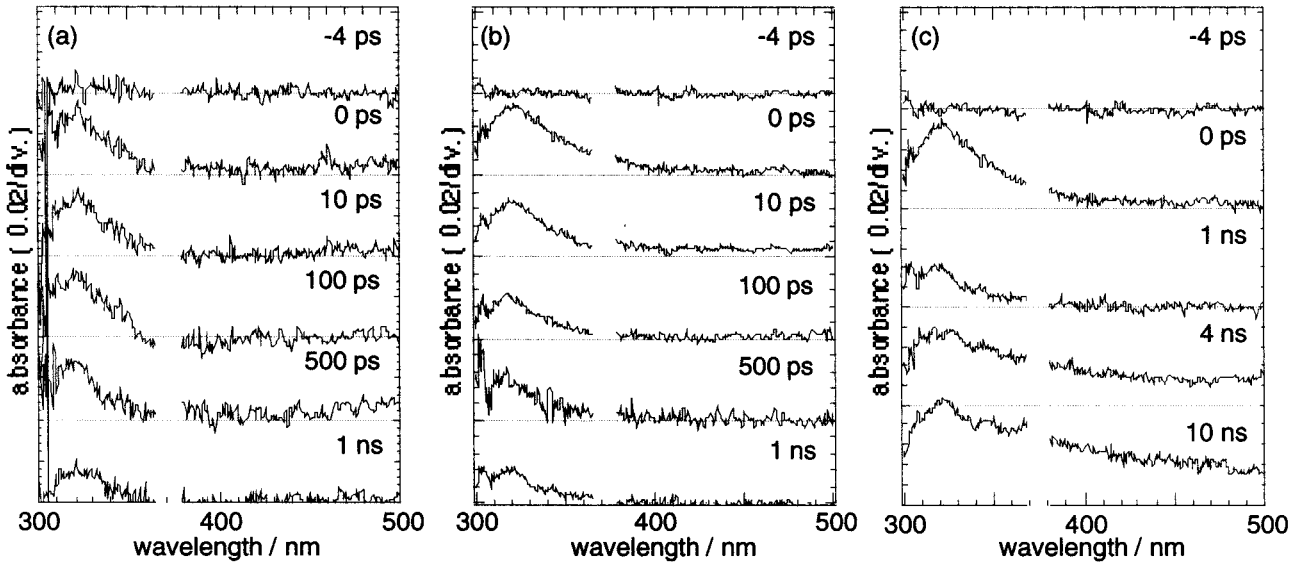

Figure 8. Time-resolved absorption spectra where the sample was liquid benzyl chloride and the F values were 6 mJ/cm^2 (a) and 90 mJ/cm^2 (b) in the picosecond time domain. Spectral change at 90 mJ/cm^2 in the nanosecond time domain is shown in (c). The times in frames represent delay times. Spectra around the wavelength of 372 nm were eliminated due to our inability to calculate them correctly as a result of the saturation of white light continuum intensity.

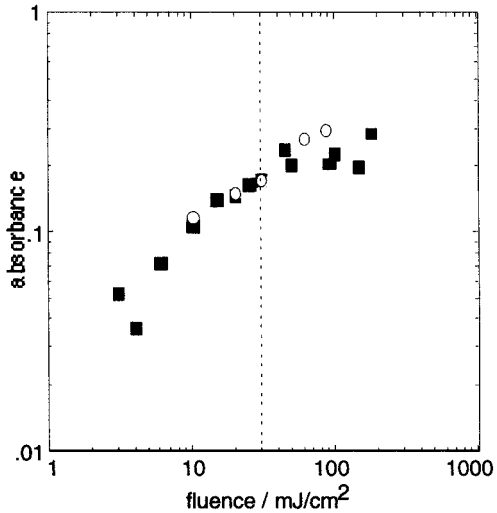

Figure 9. Fluence dependence of absorbance at 320 nm (benzyl radical). Solid squares represent the absorbance at 1 ns under femtosecond laser ablation. Open circles represent the maximum absorbance under nanosecond laser ablation. The vertical dotted line denotes the fluence threshold (30 mJ/cm^2) of femtosecond and nanosecond laser ablation.

time domain. A second broad band tailing to the longer wavelength was observed following complete decay of the initial broad band at 1 ns at $F = 90$ mJ/cm^2 > F_{th}; in contrast, nothing was observed at $F = 15$ mJ/cm^2 < F_{th}. As in the case of benzyl chloride, this phenomenon was assigned to morphological changes (see previous discussion regarding benzyl chloride).

Candidates giving rise to the initial broad absorption band are S_1 and T_1 states of toluene monomer, toluene excimer, ions, etc. The absorbance at 320 nm was plotted as a function of F value (not shown),[30] and its slope was nearly unity, suggesting that production of transient species proceeded via a one-photon process. Further, the rise and decay profile (not shown)[30] revealed an instantaneous rise at 320 nm following laser excitation. On the basis of these experimental results, the origin of absorption at shorter wavelength is mainly S_1 of toluene when the absorption band of benzene monomer[40] displaying a tail in the wavelength range is taken into consideration. On the other hand, the T_1 absorption of benzene in solution occurs at a wavelength shorter than 300 nm (the peak is at 235 nm),[40] which is thought to be similar to the case of liquid toluene. As a result, T_1 of toluene monomer does not account for the main origin of absorption observed in the wavelength range. Over the longer wavelength range, a 20-ps-long rise at 480 nm was observed. This rise was assigned to a toluene excimer formation process following rotational relaxation, diffusion and collisions after S_1 formation as the absorption peak wavelength of toluene excimer was reported to be ~550 nm.[51] When laser fluence was relatively high (Figure 10b), in addition to the transient species discussed, ions such as toluene radical cation were potentially present when efficient two-photon-absorption (10 eV) occurred due to the ionization energy of toluene in liquid phase[36] (reported to be 6.9 eV). The benzyl radical cation spectrum[52] is reported to be broad around 500 nm, which cannot be readily distinguished from other species such as S_1. Phenomena related to ions such as Coulomb explosion can be neglected as a plausible rationale for the ablation mechanism as no significant absorption at 1 ns is evident at the onset of morphological changes.

On the basis of the aforementioned discussion, we concluded that the primary transient species formed under femtosecond laser ablation of toluene are S_1 and toluene excimer. These photophysical transients played a key role in the laser ablation molecular mechanism. The absorbance at 320 nm corresponding to S_1 concentration decayed with a lifetime of several hundred picoseconds. This result is much shorter than the reported value of 34 ns.[53] This event is due to the excited states interaction in the highly concentrated S_1 state under laser ablation conditions, which enhances a nonradiative relaxation process leading to heat generation. Quantitative temperature elevation cannot be deduced directly from the spectra; however, temperature elevation velocity is estimated to be 4.3×10^{10}−4.3×10^{13} K/s from eq 3.[30] This value is reasonable for laser ablation given that Dlott et al.[8] reported that the temperature jump was on the order of 10^{12} K/s during picosecond laser ablation of a polymer doped with infrared dye molecules. We concluded that femtosecond laser ablation of toluene is induced by instantaneous heat generation resulting from the excited-state interaction between S_1.

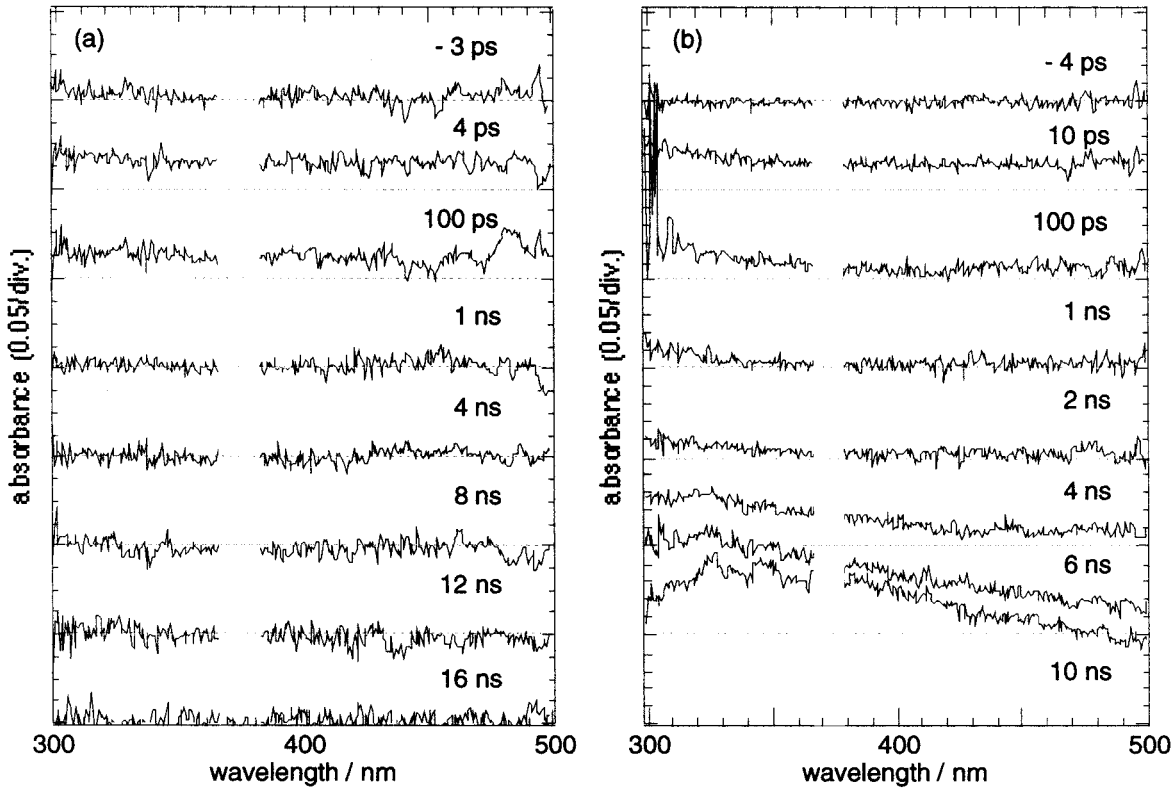

Figure 10. Time-resolved absorption spectra where the sample was liquid toluene and the laser fluences were 15 mJ/cm^2 (a) and 60 mJ/cm^2 (b). The times in frames represent delay times. Spectra around the wavelength of 372 nm were eliminated due to our inability to calculate them correctly as a result of the saturation of white light continuum intensity.

The most striking feature of time-resolved absorption spectra of liquid toluene is that no peak is observed around the wavelength of 320 nm originating from benzyl radical under any condition. This situation appears to be independent of laser fluence intensity and time of observation. This result is definitely contrary to the reaction in (1). The benzyl radical formation process from liquid toluene had remained largely unknown until the present. The most remarkable difference between nanosecond laser ablation and femtosecond laser ablation involves pulse width, which strongly indicates that benzyl radical is produced via a single transient species, of which formation time constant is on the order of picosecond to nanosecond.

In benzyl radical formation via the aforementioned pathway, a nanosecond pulse can be equivalent to sequential femtosecond pulses. On the basis of this consideration, femtosecond double-pulse excitation was conducted.[30] Figure 11 displays two transient absorption spectra, one is measured under single pulse excitation conditions (thin line, 19 ns delay between excitation1 and probe) and the second is measured under double-pulse excitation conditions (thick line, 9 ns delay between excitation1 and excitation2, 10 ns delay between excitation2 and probe). No significant spectrum was observed in the former case, whereas an absorption band, of which peak wavelength was about 320 nm, was evident in the latter case. No doubt exists that this band originates from the benzyl radical as the spectrum is in close agreement with a reference spectrum;[39] moreover, experimental results obtained for benzyl chloride also demonstrate close agreement.[27,29]

Numerous reports regarding the benzyl radical formation process in gas phase have been published. The hot molecular mechanism can be viewed as a benzyl radical formation process, where benzyl radical production is believed to occur via a highly vibrationally excited state of the electronic ground state. In the liquid phase, however, collisions between molecules are dominated in the picosecond time domain so much so that the hot molecular mechanism is unlikely as a candidate for the benzyl radical formation process. In fact, benzyl radical absorption was not observed in our experiments under conditions capable of producing such a highly vibrationally excited state, i.e., when the laser intensity was extremely high. On the other hand, Koyanagi and Uejoh[54] reported that toluene in benzene matrix at 77 and 4.4 K dissociated into benzyl radical from a higher excited triplet state. Thus, it is suggested that benzyl radical can be produced via T_1 from toluene in liquid phase. Normally, the intersystem crossing time constant is approximately 6 ns from S_1 of toluene to T_1. Additionally, the time can be shorter under laser ablation conditions due to S_1-S_1 annihilation, which

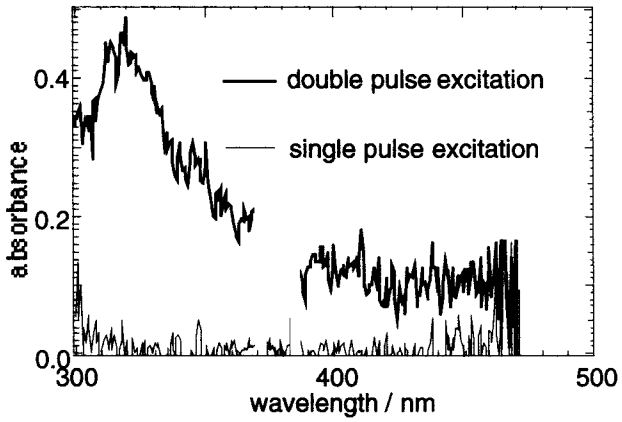

Figure 11. Absorption spectra of liquid toluene under the conditions of single and double pulse excitations. The spectrum in a thin solid line was obtained under single pulse excitation conditions; excitation 1 ← 19 ns → probe. The thick-lined spectrum was obtained under double pulse excitation conditions; excitation 1 ← 9 ns → excitation 2 ← 10 ns → probe. Laser fluences were 10 and 40 mJ/cm^2 for excitation 1 and 2, respectively.

indicates that there is insufficient time for photon absorption by T_1 when an excitation light pulse width is on the order of femtosecond as in the present case. This reason accounts for why the absorption band of benzyl radical is not observed under single pulse excitation conditions.

V. Summary

In the present investigation, we have developed several novel experimental techniques, applied them to the laser ablation study of liquids and succeeded in connecting the gap between molecular mechanisms and morphological changes. Nanosecond laser ablation clarified the correlation of thresholds with the production of benzyl radical via photochemical reactivity and not boiling point. Spectroscopy confirmed benzyl radical formation under laser ablation conditions. Finally, benzyl radical concentration necessary to induce laser ablation was estimated. On the bases of these findings, we concluded that laser ablation was induced by the photochemically produced benzyl radical. In the femtosecond laser ablation, on the other hand, the relation of the ablation thresholds between benzyl chloride and toluene was changed from that in the nanosecond laser ablation. In the spectroscopy, a benzyl radical formation was confirmed in benzyl chloride, not in toluene. The absorption spectroscopy under double pulse excitation made it clear that the radical formation processes were different between them. Then, we have concluded that the ablation mechanism of benzyl chloride was the same as the nanosecond laser ablation mechanism and that of toluene changed to photothermal mechanism. Additionally, the morphological changes were observed with a higher temporal and spatial resolution.

The success of direct correlation between the molecular mechanisms and the morphological changes is owed to the simple structure of liquids. Because of the simplicity, a model calculation can be performed with a high reliability as Garrison et al.[55] performed. In polymers, on the other hand, their structures are microscopically complex due to conformation and so on. As a result, photophysical and photochemical relaxation processes do not induce macroscopic morphological changes directly, which results in the difficulty of ablation study. On the basis of the knowledge on the ablation mechanisms of liquids, discussions on laser ablation of polymers from the viewpoint of polymer characteristics will be greatly advanced as we tried in the laser ablation mechanism of polystyrene.[56]

Acknowledgment. The authors acknowledge Mr. M. Kawao, Mr. T. Itoh, Assoc. Prof. Dr. T. Asahi, Dr. N. Ichinose, Dr. S. Kawanishi, and Dr. T. Sasuga for their collaboration, kind support and helpful discussion. This work was supported in part by Grant-in-Aids for Scientific Research from the Ministry of Education, Science, Sports and Culture of Japan (Grant Nos. are 05650924, 05640572, 07554063, 06239101, 09304067, and 10207204).

References and Notes

(1) Committee to Survey Opportunities in the Chemical Sciences, Board on Chemical Sciences and Technology, Commission on Physical Sciences, Mathematics, and Resources, National Research Council. *Oppotunities in Chemistry*; National Academy Press: Washington DC, 1985.

(2) Tamai, N.; Asahi, T.; Masuhara, H. *Chem. Phys. Lett.* **1992**, *198*, 413.

(3) Fukazawa, N.; Yoshioka, K.; Fukumura, H.; Masuhara, H. *J. Phys. Chem.* **1993**, *97*, 6753. Hashimoto, S.; Fukazawa, N.; Fukumura, H., Masuhara, H. *Chem. Phys. Lett*. **1994**, *223*, 493. Ichikawa, M.; Fukumura, H.; Masuhara, H. *J. Phys. Chem*. **1994**, *98*, 12211. Ichikawa, M.; Fukumura, H.; Masuhara, H. Koide, A.; Hyakutake, H. *Chem. Phys. Lett*. **1995**, *232*, 346. Furube, A.; Asahi, T. Masuhara, H.; Yamashita, H.; Anpo, M. *J. Phys. Chem. B.* **1999**, *103*, 3120.

(4) Honda, H.; Miura, E.; Katsura, K.; Takahashi, E.; Kondo, K. *Phys. Rev. A.* **2000**, *61*, 23201.

(5) Srinivasan, R.; Mayne-Banton, V. *Appl. Phys. Lett.* **1982**, *41*, 576.

(6) Kawamura, Y.; Toyoda, K.; Namba, S. *Appl. Phys. Lett*. **1982**, *40*, 374.

(7) Srinivasan, R.; Braren, B. *Chem. Rev*. **1989**, *89*, 1303.

(8) Chen, S.: Lee, I. Y. S.; Tolbert, W. A.; Wen, X.; Dlott. D. D. *J. Phys. Chem*. **1992**, *96*, 7178.

(9) Masuhara, H.; Hiraoka, H.; Domen, K. *Macromolecules* **1987**, *20*, 450.

(10) Hiraoka, H.; Chuang, T. J.; Masuhara, H. *J. Vac. Sci. Technol*. **1988**, *B6*, 463.

(11) Fujiwara, H.; Hayashi, T.; Fukumura, H.; Masuhara, H. *Appl. Phys. Lett*. **1994**, *64*, 2451.

(12) Masuhara, H.; Fukumura, H. *Polym. News* **1991**, *17*, 5.

(13) Fukumura, H.; Mibuka, N.; Eura, S.; Masuhara, H. *Appl. Phys*. **1991**, *A53*, 255.

(14) Fukumura, H.; Masuhara, H. *J. Photopolym. Sci. Technol*. **1992**, *5*, 223. Fukumura, H.; Takahashi, E.; Masuhara, H. *J. Phys. Chem*. **1995**, *99*, 750.

(15) Furutani, H.; Fukumura, H.; Masuhara, H. *Appl. Phys. Lett*. **1994**, *65*, 3413. Furutani, H.; Fukumura, H.; Masuhara, H. *J. Phys. Chem*. **1996**, *100*, 6871.

(16) Fukumura, H.; Masuhara, H. *Chem. Phys. Lett*. **1994**, *221*, 373.

(17) Fujiwara, H.; Nakajima, Y.; Fukumura, H.; Masuhara, H. *J. Phys. Chem*. **1995**, *99*, 11481.

(18) Fujiwara, H.; Fukumoto, H.; Hayashi, T.; Fukumura, H.; Masuhara, H. Unpublished data.

(19) Bennett, L. S.; Lippert, T.; Furutani, H.; Fukumura, H.; Masuhara, H. *Appl. Phys*. **1996**, *A63*, 327.

(20) Ikeda, N.; Nakashima, N.; Yoshihara, K. *J. Chem. Phys*. **1985**, *82*, 5285. Kajii, Y.; Obi, K.; Tanaka, I.; Ikeda, N.; Nakashima, N.; Yoshihara, K. *J. Chem. Phys*. **1987**, *86*, 6115. Nakashima, N.; Ikeda, N.; Yoshihara, K. *J. Phys. Chem*. **1988**, *92*, 4389.

(21) Brouwer, L. D.; Muller-Markgraf, W.; Troe, J. *J. Phys. Chem*. **1988**, *92*, 4905. Muller-Markgraf, W.; Troe, J. *J. Phys. Chem*. **1988**, *92*, 4914.

(22) Hippler, H.; Troe, J.; Wendelken, H. J. *J. Chem. Phys*. **1983**, *78*, 6709. Brand, U.; Hippler, H.; Lindemann, L.; Troe, J. *J. Phys. Chem*. **1990**, *94*, 6305.

(23) Lowrance, W. D.; Moore, C. B.; Petek, H. *Science* **1985**, *227*, 895.

(24) Porter, G.; Wright, F. J. *Trans. Faraday Soc*. **1955**, *51*, 1469. Porter, G.; Windsor, M. W. *Nature*, **1957**, *180*, 188. Porter, G.; Strachan, E. *Trans. Faraday Soc*. **1958**, *54*, 1595.

(25) Okamura, T.; Tanaka, I. *J. Phys. Chem*. **1975**, *79*, 2728. Fukushima, M.; Obi, K. *Chem. Phys. Lett*. **1995**, *242*, 443. Tokumura, K.; Udagawa, M.; Ozaki, T.; Itoh, M. *Chem. Phys. Lett*. **1987**, *141*, 558.

(26) Tsuboi, Y.; Hatanaka, K.; Fukumura, H.; Masuhara, H. *J. Phys. Chem*. **1994**, *98*, 11237.

(27) Tsuboi, Y.; Hatanaka, K.; Fukumura, H.; Masuhara, H. *J. Phys. Chem*. **1998**, *A102*, 1661.

(28) Hatanaka, K.; Itoh, T.; Asahi, T.; Ichinose, N.; Kawanishi, S.; Sasuga, T.; Fukumura, H.; Masuhara, H. *Appl. Phys. Lett*. **1998**, *73*, 3498.

(29) Hatanaka, K.; Itoh, T.; Asahi, T.; Ichinose, N.; Kawanishi, S.; Sasuga, T.; Fukumura, H.; Masuhara, H. *Chem. Phys. Lett*. **1999**, *300*, 727.

(30) Hatanaka, K.; Itoh, T.; Asahi, T.; Ichinose, N.; Kawanishi, S.; Sasuga, T.; Fukumura, H.; Masuhara, H. *J. Phys. Chem*. **1999**, *A103*, 11257.

(31) Zweig, A. D.; Venugopalan, V.; Deutsch, T. F. *Laser Ablation in Materials Processing: Fundamentals and Applications*; Braren, B., Dubowski, J. J., Norton, D. P. Eds.; Material Research Society: Pennsylvania, 1993; p.69.

(32) Snyder, E. M.; Wei, S.; Purnell, J.; Buzza, S. A.; Castleman, A. W., Jr. *Chem. Phys. Lett*. **1996**, *248*, 1.

(33) Campbell, E. E. B.; Ulmer, G.; Bues, K.; Hertel, I. V. *Appl. Phys*. **1989**, *A48*, 543.

(34) Watanabe, I.; Ono, K.; Ikeda, S. *Bull. Chem. Soc. Jpn*. **1991**, *64*, 352.

(35) Weast, R. C.; Lide, D. R.; Astle, M. J.; Beyer, W. H. *CRC Handbook of Chemistry and Physics*, 70th ed.; CRC Press: Boca Raton, FL, 1990.

(36) Braun, C. L.; Kato, S.; Lipsky, S. *J. Chem. Phys*. **1963**, *39*, 1645.

(37) Takemura, T.; Fujita, M.; Ohta, N. *Chem. Phys. Lett*. **1988**, *145*, 215.

(38) Pearse, R. W. B.; Gaydon, A. G. *The Identification of Molecular Spectra*; John Wiley & Sons: New York, 1976.

(39) Meisel, D.; Das, P. K.; Hug, G. L.; Bhattacharyya, K.; Fessenden, R. W. *J. Am. Chem. Soc*. **1986**, *108*, 4706.

(40) Nakashima, N.; Sumitani, M.; Ohmine, I.; Yoshihara, K. *J. Phys. Chem*. **1980**, *72*, 2226. Ikeda, N.; Nakashima, N.; Yoshihara, K. *J, Am. Chem. Soc*. **1985**, *107*, 3381.

(41) Hiratsuka, H.; Okamura, T.; Tanaka, I.; Tanizaki, Y. *J. Phys. Chem*. **1980**, *84*, 285.

(42) Hatanaka, K.; Ichinose, N.; Kawanishi, S.; Sasuga, T.; Fukumura, H.; Masuhara, H. *Abstract of 4th International Workshop on Femtosecond Technology*, 1997; p 139.
(43) Tsuboi, Y.; Fukumura, H.; Masuhara, H. *Appl. Phys. Lett*. **1994**, *64*, 2745.
(44) Bennett, H. E.; Porteus, J. O. *J. Am. Chem. Soc*. **1961**, *51*, 123.
(45) Elson, J. M.; Rahn, J. P.; Bennett, J. M. *Appl. Opt*. **1983**, *22*, 3207.
(46) Ichimura, T.; Hikida, T.; Mori, Y. *J. Phys. Chem*. **1975**, *79*, 291.
(47) Ikeda, N.; Nakashima, N.; Yoshihara, K. *J. Phys. Chem*. **1984**, *88*, 5803.
(48) Ichimura, T.; Mori, Y.; Sumitani, M.; Yoshihara, K. *J. Phys. Chem*. **1984**, *80*, 962.
(49) Gibson, G. E.; Bayliss, N. S. *Phys. Rev*. **1933**, *44*, 188.
(50) Andrews, L.; Kelsall, B. J.; Payne, C. K.; Rodig, O. R.; Schwarz, H. *J. Phys. Chem*. **1982**, *86*, 3714.
(51) Tagawa, S.; Schnabel, W. *Chem. Phys. Lett*. **1980**, *75*, 120.
(52) Hamill, W. H. *Radical Ions*; Kaiser, E. T., Kevan, L., Eds.; Wiley-Interscience: New York, 1968; p 399.
(53) Gilbert, A.; Baggott, J. *Essentials of Molecular Photochemistry*; Blackwell Science Ltd.: Oxford, 1991.
(54) Koyanagi, M.; Uejoh, K. *J. Lumin.* **1997**, *72*−*74*, 511.
(55) Garrison, B. J.; Srinivasan, R. *J. Appl. Phys*. **1985**, *57*, 2909. Zhigilei, L. V.; Kodali, P. B. S.; Garrison, B. J. *J. Phys. Chem*. **1998**, *B102*, 2845.
(56) Tsuboi, Y.; Sakashita, S.; Hatanaka, K.; Fukumura, H.; Masuhara, H. *Laser Chem.* **1996**, *16*, 167.